Available online at www.sciencedirect.com

SCIENCE DIRECT®

Catalysis Today 104 (2005) 219–224

CATALYSIS TODAY

www.elsevier.com/locate/cattod

Catalytic and electrocatalytic production of H_2 from propane decomposition over Pt and Pd in a proton-conducting membrane-reactor

George Karagiannakis, Christos Kokkofitis, Stergios Zisekas, Michael Stoukides *

Chemical Engineering Department, Aristotle University and Chem. Proc. Engineering Research Institute, U. Box 1517,
University Campus, Thessaloniki 54124, Greece

Abstract

In the present study, the C_3H_8 decomposition reaction is studied in a double-chamber proton-conducting cell-reactor. The proton conductor was a strontia–ceria–ytterbia perovskite disk of the form: $SrCe_{0.95}Yb_{0.05}O_{3-\alpha}$. The working electrode-catalyst was either Pt or Pd, in the form of a polycrystalline film. The reaction temperature varied between 923 and 1023 K and the partial pressure of propane in the feed gas was 2 kPa. The hydrogen produced by the reaction was electrochemically transported through the walls of the proton-conducting disk, to the outer reactor-chamber. The two electrodes (Pt and Pd) are compared in terms of their catalytic and electrocatalytic activities.

Keywords: Solid-state proton conductor; Propane decomposition; Propane dehydrogenation; Electrocatalytic production of hydrogen

1. Introduction

The catalytic dehydrogenation of propane is a potential method for the production of propylene, a key chemical in the polymerization and organic synthesis industries.

$$C_3H_8 \rightleftharpoons C_3H_6 + H_2, \quad \Delta H^\circ = 124\,\mathrm{kJ/mol}\,(\mathrm{at}\,298\,\mathrm{K}) \qquad (1)$$

The reaction requires high temperatures (500–700 °C) and low pressures (0.3–1 atm). At such high temperatures, however, the side-reaction of C_3H_8 thermal decomposition takes place.

$$C_3H_8 \rightarrow C_2H_4 + CH_4 \qquad (2)$$

Recently, the research interest in this reaction has increased because, in addition to propylene, hydrogen is produced and the latter tends to become the energy ‘‘currency’’ of the future. Originally, Cr-based catalysts were proposed [1], and development and improvement of these catalysts is still continuing [2–5]. Furthermore, a number of alternative catalytic systems have been tested [6–16], with the Pt–Sn-based catalysts being extensively studied [11–16] because of their high selectivity to propylene and high reaction yield.

Regardless of the catalyst used, any development in the catalytic dehydrogenation of propane has to take into account the limited conversion of reaction (1) dictated by the thermodynamic equilibrium. This reality and the increasing interest in hydrogen production from hydrocarbon fuels, led to the development of novel reactor designs and specifically, to the use of membrane-reactors [17–21]. Materials that have been used in the construction of these membrane-reactors include Pd–Ag and Pd–Ru alloys as well as silica-based membranes. Hydrogen is selectively removed from the propane stream through the solid membrane resulting to a moderate increase in propylene yield and also in producing hydrocarbon-free hydrogen.

In the last 30 years, solid electrolytes have been used in order to either study or influence the rate or the selectivity of heterogeneous catalytic reactions [22]. In these studies, oxygen ion (O^{2-}) conductors are by far the most widely used solid electrolytes and, therefore, most of the reactions studied were catalytic oxidations. Only recently, materials that exhibit proton conductivity (H^+) in the solid-state have been utilized in catalytic studies. These proton conductors

---

* Corresponding author. Tel.: +30 2310 996165; fax: +30 2310 996145.
E-mail address: stoukides@cheng.auth.gr (M. Stoukides).

0920-5861/$ – see front matter © 2005 Elsevier B.V. All rights reserved.
doi:10.1016/j.cattod.2005.03.070

could be useful in catalysis, since they can operate at temperatures in which many hydro- and dehydrogenation reactions take place [23].

As an example, let us consider the dehydrogenation reaction:

$$A \leftrightarrow B + H_2 \tag{3}$$

which is employed for the production of high purity hydrogen. In a conventional industrial process, a step of H_2 separation from the reaction mixture (A, B, H_2) is required. However, if we utilize a double-chamber proton-conducting electrochemical reactor the same reaction could take place as follows:

$$A \leftrightarrow B + H_2$$

$$H_2 \leftrightarrow 2H^+ + 2e^- \text{ (anodic electrode)} \tag{4}$$

$$2H^+ + 2e^- \leftrightarrow H_2 \text{ (cathodic electrode)} \tag{5}$$

The significant advantage that such an electrochemical reactor could offer is that the dehydrogenation reaction and the subsequent separation of hydrogen from the reaction mixture occur at the same time. The catalytic reaction takes place at the anode, while high purity H_2 is recovered at the cathode.

One important difference between an electrochemical reactor and a conventional membrane-reactor is that in the latter, the driving force for the removal of hydrogen is the difference in the partial pressure of hydrogen at the two sides of the membrane. In the proton-conducting electrochemical reactor, the driving force is the difference in the electrochemical potential of protons at the two sides of the solid-state proton conductor. Therefore, by using an external power source (e.g. a galvanostat or a potentiostat), it is possible to increase, decrease or even reverse the proton flux, if desirable.

In the present work, the reaction of propane dehydrogenation was examined in two identical electrochemical reactors, one with Pt and the other with Pd as working (anodic) electrodes. The catalytic and electrocatalytic activities of the two metals were evaluated and compared.

2. Experimental

A schematic diagram of the double-chamber reactor cell, used in the present study, is shown in Fig. 1. The proton conductor was a strontia–ceria–ytterbia perovskite disk of the form: $SrCe_{0.95}Yb_{0.05}O_{3-\alpha}$ (SCY). The procedure followed for the construction of the SCY disk was that described by Iwahara et al. [24]. The cylindrical SCY disk of 24 mm diameter and 1.5 mm thickness was sealed at the bottom of a 150 mm long ceramic tube (16 mm i.d., 19 mm o.d.). The sealing material was a $BaO–SiO_2$ glass. The ceramic tube was enclosed in a 20 cm long, closed at its bottom end, quartz tube (37 mm ID, 40 mm OD).

A porous Ag film was deposited on the outside surface of the SCY disk and served as the cathodic electrode. Similarly, a Pt or Pd film was deposited on the inside surface of the SCY disk and served as the anodic electrode (catalyst). Prior to the experiments, the electrodes were exposed to an air stream for 1 h at 800 °C. A more detailed description of the preparation of the electrodes can be found elsewhere [25]. The catalyst loadings for the Pt and Pd porous films were $m_{Pt} = 30$ mg and $m_{Pd} = 90$ mg, respectively. SEM photographs showed an average particle size of approximately 2 μm for the Pt and 5 μm for the Pd crystallites. Using these crystallite sizes, the total surface area for Pt electrode was approximately 40 cm^2, while the respective value for Pd was estimated at 90 cm^2. Additionally, the superficial surface area of both Pt and Pd electrodes was 1.5 cm^2. The C_3H_8 containing gas was flowing over the anode (Pt or Pd electrode), where H_2 was produced. Hydrogen then, was electrochemically-transported – in the form of H^+ – via the solid electrolyte from the anode to the cathode (Ag electrode), where gaseous H_2 was formed.

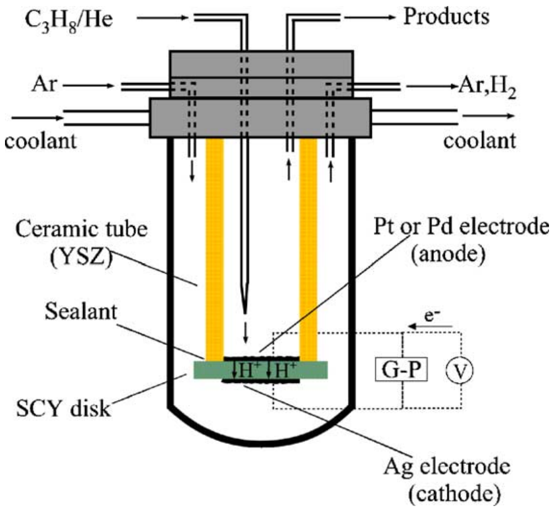

Fig. 1. Schematic description of the double-chamber cell-reactor.

Analysis of the inlet and outlet gases was performed by on-line gas chromatography, using two chromatographs, one for each chamber of the reactor cell. The inner chamber gas composition was monitored with the aid of a SHIMADZU GC-14B chromatograph equipped with a Molecular Sieve 13X and a Porapak QS column. The concentration of H_2 in the outlet chamber was measured by an HP 5890 Series 2 chromatograph, equipped with a Molecular Sieve 5A column. Constant currents and voltages across the cell were imposed using a 2053 AMEL Galvanostat–Potentiostat.

3. Results and discussion

The reaction temperature varied between 923 and 1023 K while the total pressure was 1 atm. The reaction mixtures were prepared using C_3H_8 gas diluted in He. The partial pressure of propane at the reactor inlet was 2 kPa. The reactants were introduced into the inner chamber, i.e.

over the anodic electrode, at a total flowrate of 20–40 cm^3 (STP)/min. In addition to propane, the inlet stream contained water vapor at low concentration ($P_{H2O} = 0.2$–0.5 kPa). The presence of water vapor ensures and maintains high proton conductivity of the SCY disk [26,27]. Pure Ar was introduced over the anodic electrode, i.e. in the space between the ceramic and the quartz tube, at a flow rate of 20–40 cm^3 (STP)/min. All catalytic results were obtained after, approximately, 24 h on stream, unless otherwise stated.

The products observed, under both open and closed-circuit operation, were C_3H_6, H_2, CH_4, C_2H_4, CO, CO_2 and in some cases, minor quantities of C_2H_6. The formation of CO and CO_2 is attributed to shift reactions, due to the presence of water vapor in the system.

$$C_xH_y + xH_2O \leftrightarrow xCO + (2x + y)/2H_2 \quad (6)$$

$$CO + H_2O \leftrightarrow CO_2 + H_2 \quad (7)$$

Thus, additional amounts of H_2 – apart from those formed via the propane dehydrogenation reaction – are produced via reactions (6) and (7).

3.1. Propane decomposition on Pt

The data of Figs. 2 and 3 have been obtained under open-circuit conditions (zero current through the cell). In Fig. 2, the total propane decomposition rate and the rate of H_2 formation are presented as a function of the reaction temperature. As expected, both rates increase with temperature. The total decomposition rate increases faster than H_2 formation, because at high temperatures, the thermal decomposition of propane becomes the dominant reaction. This is presented more clearly in Fig. 3, where the dependence of the products selectivity on the reaction temperature is shown. As the temperature increases, a significant decrease of C_3H_6 selectivity is observed, and at the same time the selectivity to C_2H_4 and CH_4 increases considerably. Additionally, the decrease of the CO_x selectivity indicates that the impact of shift reactions on the overall reaction scheme is less significant at higher temperatures. The selectivity to H_2 was calculated to be approximately 33% at 923 K. As the reaction temperature increased, the H_2 selectivity decreased significantly to reach a value of 12% at 1023 K.

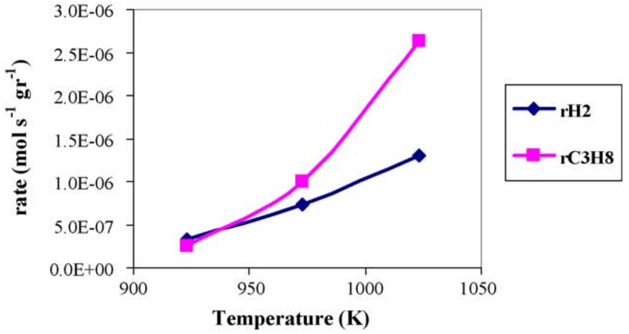

Fig. 2. Dependence of propane decomposition and hydrogen production rates on the reaction temperature under open-circuit operation on Pt ($P_{C_3H_8,inlet} = 2$ kPa).

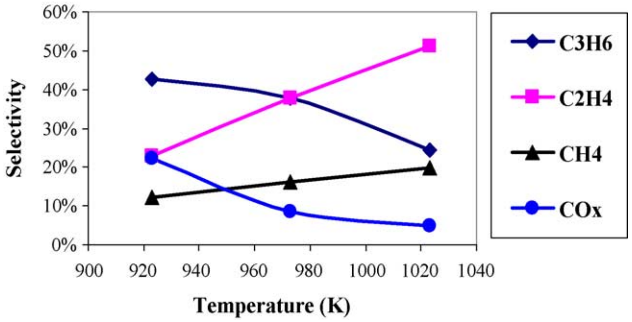

Fig. 3. Dependence of products selectivity on the reaction temperature under open-circuit operation on Pt ($P_{C_3H_8,inlet} = 2$ kPa).

It should be mentioned that, according to previous studies on propane dehydrogenation over Pt-based catalysts [11–16], the presence of Sn as an additive is required in order to avoid rapid catalyst deactivation due to carbon deposition. Contrary to these studies, insignificant catalytic deactivation was observed in the present study. This is partially attributed to the relatively low inlet partial pressure of propane ($P_{C_3H_8} = 2$ kPa) employed here as opposed to partial pressures of the order of 20–30 kPa that were utilized in previous works. Another possible explanation could be the presence of the solid electrolyte, which plays the role of the catalyst support. Especially with pure oxygen ion conductors, it has been observed that because of the high mobility of the oxygen ion, carbon deposition is substantially diminished [28,29]. The solid electrolyte used in this study is a proton conductor but under the conditions employed here, it exhibits considerable oxygen ion conductivity as well [30].

Figs. 4 and 5 contain data obtained with the cell operating under closed-circuit. In Fig. 4, the reaction rates of hydrogen, propylene, ethylene and methane formation are presented as a function of the imposed current. The imposed current is expressed as the equivalent faradaic molar flow of

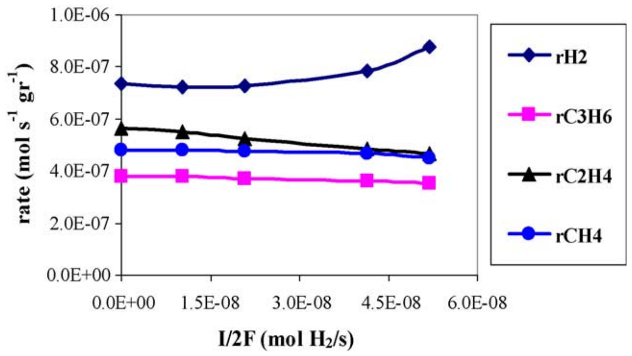

Fig. 4. Dependence of products rates on the imposed current on Pt ($P_{C_3H_8,inlet} = 2$ kPa, $T = 973$ K).

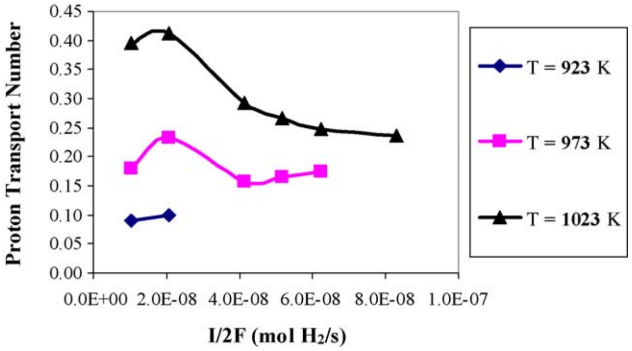

Fig. 5. Dependence of the proton transport number (PTN) on the imposed current for various reaction temperatures on Pt ($P_{C_3H_8,inlet}$ = 2 kPa).

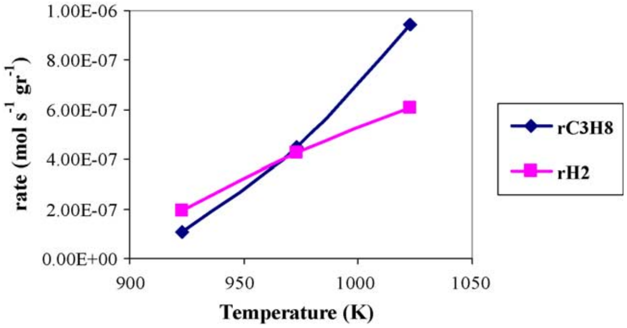

Fig. 6. Dependence of propane decomposition and hydrogen production rates on the reaction temperature under open-circuit operation on Pd ($P_{C_3H_8,inlet}$ = 2 kPa).

protons. The reaction temperature is constant at T = 973 K. It can be seen that there is no significant effect of the imposed current on any of the rates of these components. A slight increase observed in H_2 production is solely attributed to the positive effect of the current in the shift reactions (6) and (7). Similar to 973 K, the effect of current on the reaction rates was also negligible at the other two temperatures examined, i.e. 923 and 1023 K. In terms of the overall propane decomposition rate, there was no significant difference between open-circuit and closed-circuit values.

The efficiency of the imposed current, i.e. how much of the imposed current is actually effective in transferring H_2 – in the form of protons – from the reaction chamber to the outer chamber (see Fig. 1), was also examined. The proton transport efficiency can be expressed by proton transport number (PTN), which in the present experiments can be defined as:

$$\mathrm{PTN} = \frac{\text{rate of hydrogen pumped to the outer chamber}}{\mathrm{I/2F}} \qquad (8)$$

In Fig. 5, the dependence of PTN on the imposed current and on the reaction temperature is presented. It is clear that the PTN numbers are far from unity, i.e. the solid electrolyte is not a pure proton conductor, at least under the conditions of the present study. Proton transference numbers reported in the literature for SCY vary considerably [30–33]. This is because the PTN of the SCY depends not only on temperature but also on the composition of the gas to which the electrolyte surface is exposed and on the imposed current density. The work of Hamakawa et al. [33], shows that SCY is a pure H^+ conductor when exposed to H_2 on one side and Ar on the other, but becomes a mixed conductor when O_2 is cofed with Ar. On the other hand, if hydrogen is replaced by methane, the PTN drops significantly and may attain values as low as 0.4 or 0.3 [30]. Fig. 5 shows that the higher the temperature, the higher the value of the proton transport efficiency. This is attributed to the fact that H_2 production increases with temperature, causing a subsequent increase to the PTN of the solid electrolyte. Another interesting observation is that in all three reaction temperatures, there is a maximum PTN for a value of the imposed current I = 4 mA. The maximum value of PTN was approximately 0.4, attained at T = 1023 K and I = 4 mA.

3.2. Propane decomposition on Pd

The experimental procedure and the reaction conditions employed in the case of Pd electrodes were the same as those for Pt. Similarly, the products observed were the same as with Pt. The only difference is that the data presented for Pd at the lowest reaction temperature (T = 923 K) were obtained after only a few hours on stream, while in the experiments on Pt all data were taken after approximately 24 h on stream. The reason for this difference is explained below.

Figs. 6 and 7 contain open-circuit results. In Fig. 6, the total propane decomposition rate and the rate of H_2 formation are plotted versus temperature. Again, both rates increase with temperature. Similar to Fig. 3, Fig. 7 shows the effect of reaction temperature on products selectivity. A comparison between the two catalysts leads to the following observations:

(a) Both, reaction rates and products selectivity, seem to have an almost identical dependence on the reaction temperature.
(b) The reaction rates are higher in the case of Pt. This is expected because Pt is considered to be the best catalyst for propane decomposition.

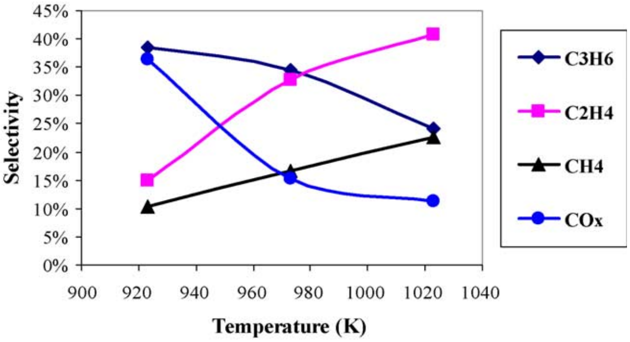

Fig. 7. Dependence of products selectivity on the reaction temperature under open-circuit operation on Pd ($P_{C_3H_8,inlet}$ = 2 kPa).

(c) Pd seems to be more selective to shift reactions (CO_x formation).
(d) The values of H_2 selectivity in the case of Pd were found to be slightly higher than the respective ones over Pt. At 923 K, the selectivity to H_2 was approximately 45%, while at 1023 K it dropped to 16%.

Another difference between the two catalysts is that with Pd and at $T = 923$ K, severe catalytic deactivation took place after exposure of the catalyst on the reaction mixture for 24 h. This can be attributed to carbon deposition on the Pd surface. The only products observed were CH_4, H_2, traces of C_2H_4 and carbon deposited on the surface of the electrode. Compared to the stable catalytic activity experiments, the rate of H_2 formation was unusually high and the respective one for CH_4 was one order of magnitude lower. The two dominating reactions are possibly the following:

$$C_3H_8 \leftrightarrow 3C + 4H_2 \tag{9}$$

$$C_3H_8 \leftrightarrow 2CH_4 + C \tag{10}$$

The present experimental results indicate that for every C_3H_8 molecule consumed in reaction (10), five C_3H_8 molecules are consumed in reaction (9).

It must be noted that upon imposing an electrical current through the solid electrolyte (in the direction that corresponds to protons ‘‘pumped’’ away from the catalyst), the catalytic activity was partially recovered. The rates of CH_4, H_2 and C formation decreased while C_3H_6 formation started taking place again. The higher the value of the imposed current, the higher is the rate of C_3H_6 production. This behavior is shown in Fig. 8a and b. This ‘recovery of catalytic activity’ was interrupted upon interruption of the imposed current. A possible explanation to this interesting observation could be the severe electrochemical modification of the catalytic activity. It is obvious that after substantial carbon deposition on the Pd surface, a considerably different behavior from that of ‘‘clean’’ Pd should be expected. This effect of ‘recovery of catalytic activity’ is undoubtedly a matter that needs further investigation.

In Fig. 9, the dependence of the rates of hydrogen, propylene, ethylene and methane formation are presented, as a function of the imposed current through the cell. The imposed current is expressed as the equivalent faradaic molar flow of protons. The only product affected by the imposed current is hydrogen. This observation indicates that the increase of H_2 formation with the imposed current is solely attributed to changes in the shift reactions (6) and (7). As far as the overall propane decomposition rate is concerned, at the maximum value of the imposed current, a 15% increase of the open-circuit rate was observed. Fig. 10 shows the effect of current on PTN. In general, the PTN values observed here are quite higher than those on Pt, reaching values of the order of 0.60 at $T = 973$–1023 K. The odd behavior at $T = 923$ K is attributed to the dramatic

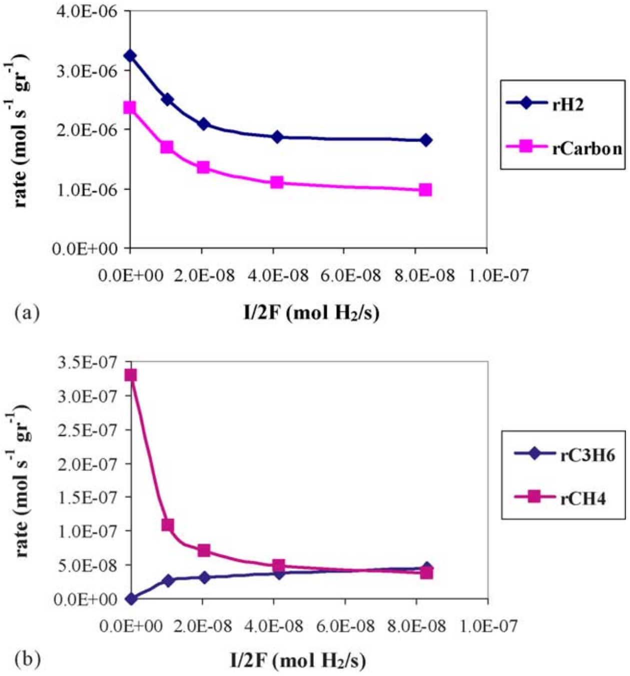

Fig. 8. (a) Effect of the imposed current on H_2 production and carbon deposition in the case of deactivated Pd catalyst ($P_{C_3H_8,inlet} = 2$ kPa, $T = 923$ K). (b) Effect of the imposed current on C_3H_6 and CH_4 production in the case of deactivated Pd catalyst ($P_{C_3H_8,inlet} = 2$ kPa, $T = 923$ K).

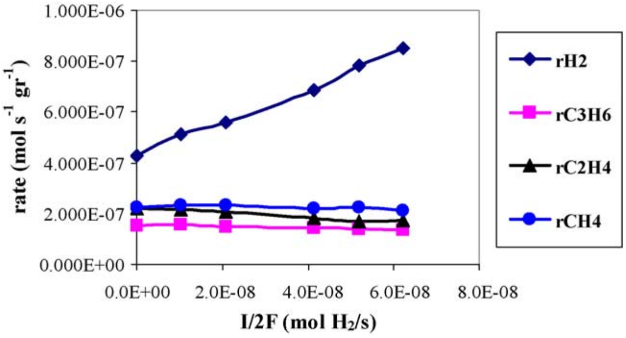

Fig. 9. Dependence of products rates on the imposed current on Pd ($P_{C_3H_8,inlet} = 2$ kPa, $T = 973$ K).

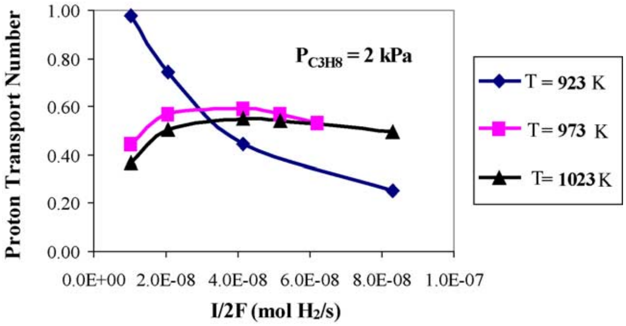

Fig. 10. Dependence of the PTN on the imposed current for various reaction temperatures on Pd ($P_{C_3H_8,inlet} = 2$ kPa).

changes in the catalytic activity accompanied by very high rates of hydrogen production, as described previously. It is notable that at the lowest value of the imposed current ($I = 2$ mA), almost pure proton conduction is observed (PTN = 0.98). Nevertheless, as the imposed current increases and the catalyst recovers its activity, a drastic drop of the PTN values occurs.

4. Conclusions

Comparing the two catalysts in terms of their catalytic activities, it was found that platinum is superior to palladium yielding to higher rates of propane decomposition. As far as the products selectivity is concerned, Pt shows a slightly higher selectivity to propylene while shift reactions (CO_x formation) are more favored on Pd. Palladium exhibits severe deactivation after remaining for approximately 24 h on stream, at $T = 923$ K. The only products observed in this case were carbon, methane and hydrogen.

On the other hand, when electrical current was imposed through the reactor cell – so that hydrogen was being transferred from the inner to the outer chamber – the only reaction rates affected were those of H_2, CO and CO_2 formation. These three products rates, generally, increased with the imposed current. The increase is much stronger with Pd electrodes. This observation indicates that only the side-reactions, due to the water-gas presence in the system, are affected by the electrocatalytic operation of the cell. When severe deactivation of Pd occurred, ''proton pumping'' away from the catalyst resulted in partial recovery of its previous activity. This recovery stopped as soon as the imposed current was interrupted.

Future work will focus on efforts to increase the proton efficiency (PTN) of the cells. A possible way to achieve this is by introducing small amounts of gaseous H_2 in the feed gas. According to previous studies [11,13,15], presence of gaseous H_2 could decrease or even eliminate the problem of catalyst deactivation. Preliminary work in our laboratory indicates that at lower temperatures, H_2 presence increases both propylene selectivity and PTN. On the other hand, increasing the concentration of hydrogen would lead to a decrease in the rate of propane dehydrogenation according to reaction (1). Work towards determining the optimal hydrogen content so that both, PTN increases and the rate of propane decomposition remains acceptably high, is currently in progress.

Acknowledgements

We gratefully acknowledge financial support of this research by the European Union (GROWTH Programme, GRD1-2001-40315). We also thank Dr. Lipilin who prepared in his laboratory (Ekarerinenburg, Russia) and provided us with the sealing glass material.

References

[1] F.E. Frey, W.F. Huppke, Ind. Eng. Chem. 25 (1933) 54.

[2] S. De Rossi, G. Ferraris, S. Fremiotti, E. Garrone, G. Ghiotti, M.C. Campa, V. Indovina, J. Catal. 148 (1994) 36.

[3] L.R. Mentasty, O.F. Gorriz, L.E. Cadus, Ind. Eng. Chem. Res. 38 (1999) 396.

[4] M. Alcantara-Rodriguez, E. Rodriguez-Castellon, A. Jimenez-Lopez, Langmuir 15 (1999) 1115.

[5] F.J. Perez-Reina, E. Rodriguez-Castellon, A. Jimenez-Lopez, Langmuir 15 (1999) 8421.

[6] T.-K. Cheung, F.C. Lange, B.C. Gates, J. Catal. 159 (1996) 99.

[7] Y. Ono, Catal. Rev. Sci. Eng. 34 (1992) 179.

[8] F. Solymosi, R. Nemeth, L. Ovari, L. Egri, J. Catal. 195 (2000) 316.

[9] K. Otsuka, S. Kobayashi, S. Takenaka, Appl. Catal. A: Gen. 210 (2001) 371.

[10] K. Otsuka, Y. Shigeta, S. Takenaka, Int. J. Hydrogen Energy 27 (2002) 11.

[11] D. Akporiaye, S.F. Jensen, U. Olsbye, F. Rohr, E. Rytter, M. Rønnekleiv, A.I. Spjelkavik, Ind. Eng. Chem. Res. 40 (2001) 4741.

[12] G.A. Sault, A. Martino, S.J. Kawola, E. Boespflug, J. Catal. 191 (2000) 474.

[13] P. Meriaudeau, A. Thangaraj, J.F. Dutel, C. Naccache, J. Catal. 167 (1997) 180.

[14] G.C. Bond, X. Lin, J. Catal. 169 (1997) 76.

[15] A.O. Bariås, A. Holmen, A.E. Blekkan, J. Catal. 158 (1996) 1.

[16] M. Larsson, M. Hultén, A.E. Blekkan, B. Andersson, J. Catal. 164 (1996) 44.

[17] Z.D. Ziaka, R.G. Minet, T.T. Tsotsis, AIChE J. 39 (1993) 526.

[18] Z.D. Ziaka, R.G. Minet, T.T. Tsotsis, J. Membr. Sci. 77 (1993) 221.

[19] J.P. Collins, R.W. Schwartz, R. Sehgal, T.L. Ward, C.J. Brinker, G.P. Hagen, C.A. Udovich, Ind. Eng. Chem. Res. 35 (1996) 4398.

[20] M. Sheintuch, R.M. Dessau, Chem. Eng. Sci. 51 (1996) 523.

[21] O. Wolfrath, L. Kiwi-Minsker, A. Renken, Ind. Eng. Chem. Res. 40 (2001) 5234.

[22] M. Stoukides, Cat. Rev. Sci. Eng. 42 (2000) 1.

[23] H. Iwahara, H. Uchida, S. Tanaka, J. Appl. Electrochem. 16 (1986) 663.

[24] H. Iwahara, T. Esaka, H. Uchida, N. Maeda, Sol. St. Ionics 3–4 (1981) 79.

[25] G. Marnellos, S. Zisekas, M. Stoukides, J. Catal. 193 (2000) 80.

[26] N. Bonanos, in: Proceedings of the fourteenth Riso International Symposium on Materials Science, Denmark, 1993.

[27] H. Iwahara, T. Shimura, H. Matsumoto, Electrochemistry 68 (1999) 154.

[28] D. Eng, M. Stoukides, Catal. Lett. 9 (1991) 47.

[29] H. Alqahtany, D. Eng, M. Stoukides, J. Electrochem. Soc. 140 (1993) 1677.

[30] P.-H. Chiang, D. Eng, M. Stoukides, Solid State Ionics 61 (1993) 99.

[31] S. Hamakawa, T. Hibino, H. Iwahara, J. Electrochem. Soc. 141 (1994) 1720.

[32] N. Bonanos, B. Ellis, M.N. Mahmood, Solid State Ionics 28-30 (1988) 579.

[33] S. Hamakawa, T. Hibino, H. Iwahara, J. Electrochem. Soc. 140 (1993) 459.